New Approaches for Nonstationary Cluster-based and TFCE inference

Reza Salimi-Khorshidi[1], Stephen M. Smith[1], Thomas E. Nichols[1,2]

[1]FMRIB Centre, Oxford University, Oxford, UK;

[2]GlaxoSmithKline Clinical Imaging Centre, London, UK.

Introduction

In neuroimaging, cluster-based inference has generally been found to be more powerful than voxel-wise inference [Friston et al. 96]. However standard cluster-based methods assume stationarity (constant smoothness across space), while under nonstationarity, clusters tend to be larger in smooth regions, making false positive risk spatially variant. Hayasaka et al. [2004] proposed a Random Field Theory (RFT) based nonstationarity adjustment for cluster inference and validated the method in terms of controlling the overall family-wise false positive rate. The RFT-based methods, however, have never been directly assessed in terms of homogeneity of local false positive risk.

In this work we propose a new cluster size adjustment that accounts for local smoothness based on local empirical cluster size distributions and a two-pass permutation method. We also propose a new approach to measure homogeneity of local false positive risk, and use this method to compare the RFT-based and our new empirical adjustment methods. We apply these techniques to both cluster-based and a related inference, threshold-free cluster enhancement (TFCE) [Smith and Nichols 2008]. Using simulated and real data we confirm the expected heterogeneity in false positive risk with unadjusted cluster inference, find that RFT-based adjustment does not fully eliminate heterogeneity, that our proposed empirical adjustment dramatically increases the homogeneity and that TFCE inference is in any case generally robust to nonstationarity.

Methods

After fitting the general linear model (GLM) to each voxel's observation time-series, the standardised residual error ($S_{i,t}$ for voxel i at time t) is used to estimate the underlying smoothness/roughness of the image. Two RFT-based methods are employed in order to provide the analysis with roughness estimates per voxel (RPV): Kiebel's (Eq.1) [Kiebel et al 1999] and Jenkinson's (Eq.2) [Flitney and Jenkinson 2000; Nichols 2008] methods that are based on the spatial derivative and spatial correlation of the residual error, respectively. Calculating the cluster sizes in RPV units and using them in cluster-based or TFCE inference can adjust the inference for nonstationarity.

Our empirical approach records the (nonzero) cluster size and TFCE value at each voxel for each permutation, and then creates an average (nonzero) cluster size or TFCE map over permutations. In a 2nd run through the data (with the same permutations) this map is used to normalise cluster size and TFCE to account for nonstationarity (see Eq.3 and 4). We call this summary statistic from the first run empirical cluster-size or TFCE per voxel (ECSPV or ETPV, respectively).

Using null data, the output false positive rate (P-value) volume is expected to be sampled from the uniform distribution U(0,1). It can be shown that both the expected mean and standard deviation of the $-\log_{10}(P)$ histogram is 0.43. Thus the deviation of the spatial variation of cluster-related inference's $-\log_{10}(P)$ is utilised in order to assess different adjustments' performance. This assessment is summarised in terms of the mean and coefficient of variation (CV) of the output $-\log_{10}(P)$ histogram.

Results

The adjustment techniques are applied to both real (FMRI and VBM) and simulated (stationary and nonstationary) data. Summary performance measures on the null data are plotted in Figs. 2 and 3 as a function of the smoothness pattern for null simulated and real data, respectively. In Fig. 4, each adjustments' performance is evaluated by employing the area under the ROC curve (AUC) in percentage (0-100% for 0-1). Note that run1 and run2 represent no-empirical and empirical adjustments, robust represents the estimation without outlier observations, E in Eq.3 is the histogram normalization parameter, and rpv0 and rpv1 represent the no-adjustment and Jenkinson's method.

Conclusions

In this study, different methods are proposed for adjusting cluster-related inferences for nonstationarity. The results show that there is a substantial variation in cluster-based inference's false positive rate over space in simulated, real VBM and real FMRI data, that adjustments cannot completely correct, however, there is an improvement after correction. RFT-based adjustments result in very similar (close to identical) results, which is more sensitive than the empirical adjustment. The main shortcoming of using ECSPV is the the censoring (which occurs when the value of an observation is only partially known) caused by the use of cluster information in order to characterize each voxel. However, TFCE inference is very robust to spatial variation of the smoothing, and does not necessarily require any adjustment (according to Fig.2-4). These results support TFCE as a new powerful inference scheme for neuroimaging analyses.

(1)

$$\lambda_{i,d} = \frac{\nu-2}{\nu-1}\cdot\frac{1}{M}\sum_{t=1}^{M}\left(\frac{\partial S_{it}}{\partial x_d}\right)^2$$

$$\sigma^2_{i,d} = \frac{1}{2\lambda_{i,d}}$$

$$RPV_{i,d} = (8\cdot\ln(2))^{-1/2}\cdot\sigma_{i,d}^{-1}$$

$$RPV_i = \prod_{d=1}^{D} RPV_{i,d}.$$

(2)

$$S_i^2 = \frac{1}{M}\sum_{t=1}^{M} {S_{i,t}}^2$$

$$SS_{i,d} = \frac{1}{M}\sum_{t=1}^{M}(S_{i+_d,t}\cdot S_{i,t})$$

$$\sigma^2_{i,d} = \left(4\cdot\ln\left(\frac{S_i^2}{SS_{i,d}}\right)\right)^{-1}$$

$$RPV_{i,d} = (8\cdot\ln(2))^{-1/2}\cdot\sigma_{i,d}^{-1}$$

$$RPV_i = \prod_{d=1}^{D} RPV_{i,d}.$$

(3)

$$ECSPV(v) = \left(\frac{\sum_{i=1}^{N_v} S_i(v)^E}{N_v}\right)^{1/E}$$

$$S_C^{vn} = \sum_{v\in C}\frac{1}{ECSPV(v)}$$

(4)

$$ETPV(v) = \frac{\sum_{i=1}^{N_v} TFCE_i(v)}{N_v}$$

$$TFCE^N(v) = \frac{TFCE(v)}{ETPV(v)}$$

References

[1] Flitney & Jenkinson (2000), 'Cluster analysis revisited.', Tech Report, FMRIB Centre, University of Oxford.

[2] Friston et al (1996), 'Detecting activations in PET and FMRI: levels of inference and power'. NeuroImage, vol 4, pp.223–235

[3] Hayasaka et al (2004), 'Nonstationary cluster-size inference with random field and permutation methods.', Neuroimage, vol. 22, no. 2, pp. 676-87.

[4] Kiebel, S.J. (1999), 'Robust smoothness estimation in statistical parametric maps using standardized residuals from the general linear model.', Neuroimage, vol. 10, no. 6, pp. 756–66.

[5] Nichols (2008), 'Cluster analysis revisited - again: Implementing nonstationary cluster size inference.', Tech Report, FMRIB Centre, University of Oxford.

[6] Smith & Nichols (2009), 'Threshold-free cluster enhancement: addressing problems of smoothing, threshold dependence and localisation in cluster inference.', Neuroimage, vol. 44, no. 1, pp. 83-98.

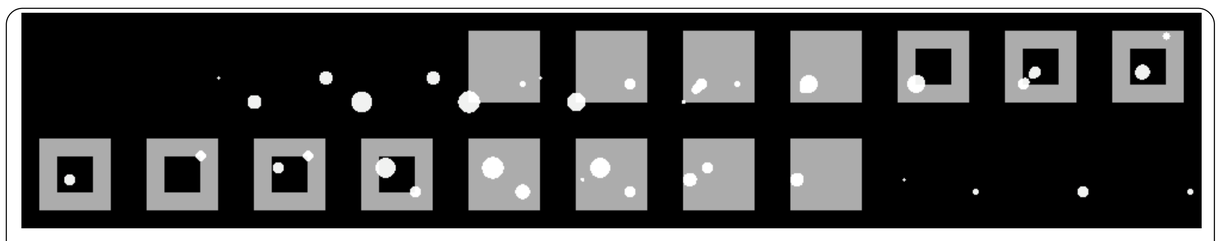

Figure 1: The simulated *signal* (white blobs) for the ROC analyses overlaid on the map of the three smoothing regions (the outer layer is smoothed with σ1 encloses a middle layer (shown in gray) smoothed with σ2 , which encircles a core smoothed with σ3; referred to as $\sigma_1\sigma_2\sigma_3$). This signal is multiplied by an SNR and then added to the Gaussian noise that is smoothed with different extents at each of these three regions.

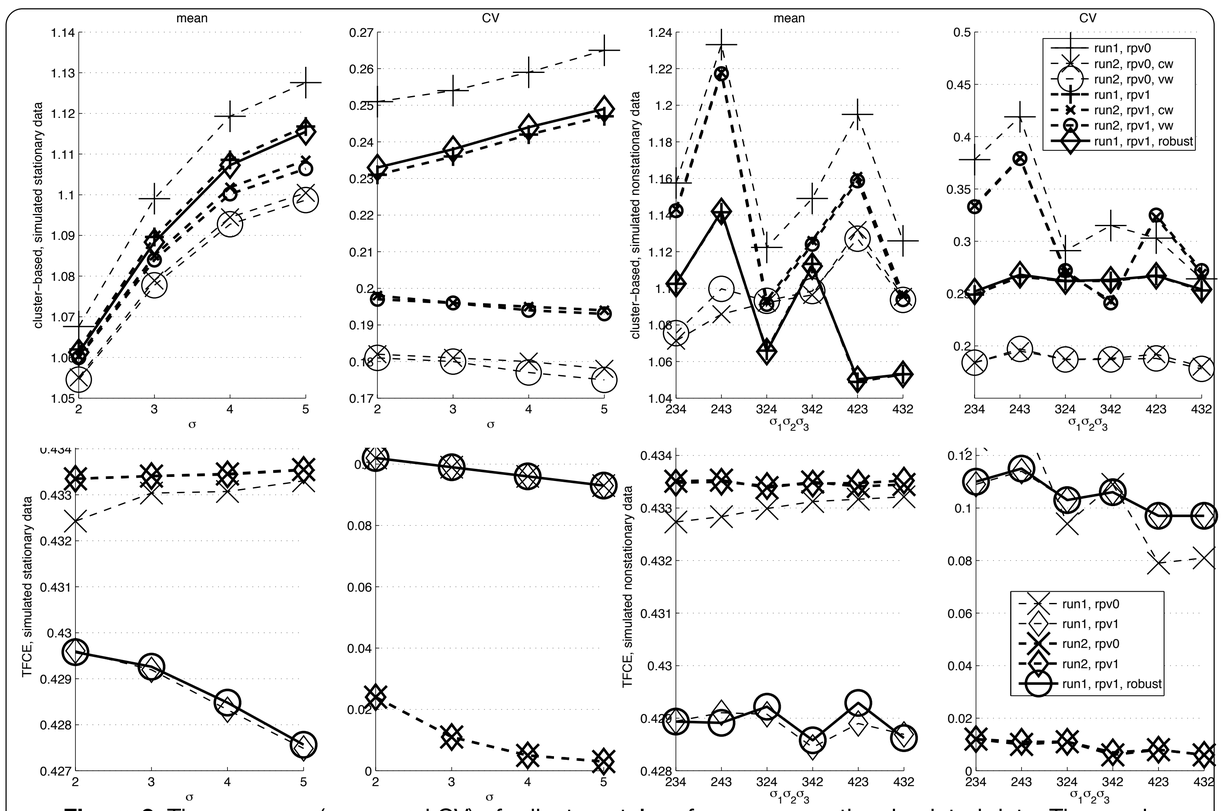

Figure 2: The summary (mean and CV) of adjustments' performances on the simulated data. The x-axis represents the smoothing extent/arrangement for stationary/nonstationary data.

Figure 3: The summary (mean and CV) of adjustments' performances on the simulated stationary and nonstationary data. The x-axis represents the smoothing extent/arrangement for stationary/nonstationary data.

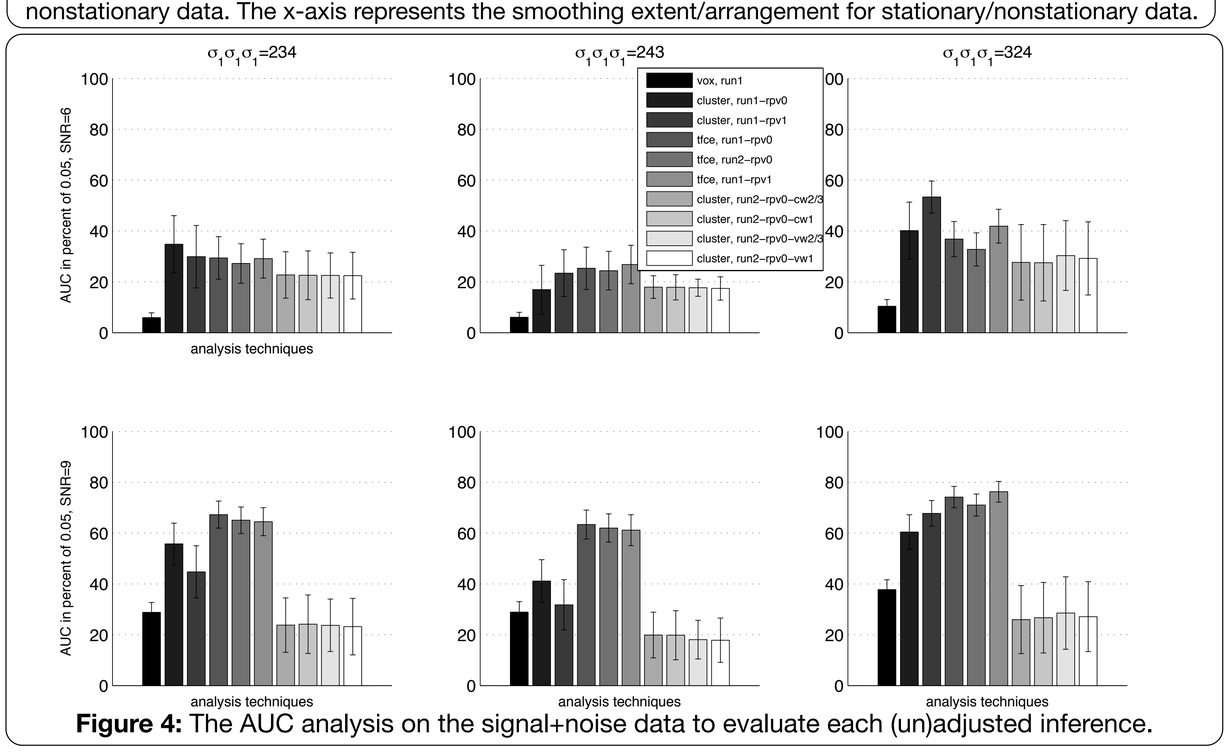

Figure 4: The AUC analysis on the signal+noise data to evaluate each (un)adjusted inference.